SCIENTIFIC Publishing Limited

New Energy Exploitation and Application

http://ojs.ukscip.com/index.php/neea

Article

Hybrid Operating Mode Management to Maximize the Service Life of Electrolyzers Running on Renewables

Rim Abdallah , Anne-Lise Gehin and Jean-Yves Dieulot *

CRIStAL - Research center in Computer Science, Signal and Automatic Control of Lille UMR 9189 CNRS, University of Lille, 59000 Lille, France

* Correspondence: jean-yves.dieulot@univ-lille.fr

Received: 4 July 2024; **Revised:** 5 July 2024; **Accepted:** 12 December 2024; **Published:** 16 December 2024

Abstract: The service life of equipment is generally linked to degradation factors depending on its operating conditions, including the rate of use and the frequency of the switching modes. The novel operating mode management proposed in this paper takes into account equipment lifetime in addition to all the previously mentioned requirements. This algorithm does not rely only on real-time data, as is traditionally presented in the literature, but also integrates predictive operating data. Therefore, it can be considered as a hybrid operating mode management as it embeds both predictive and event data, which yields improved results with respect to traditional event-driven management. This allows to optimize a criterion over a finite horizon, and, hence, an optimal sequence of the switching times of the different components of an energy system are generated. While the proposed approach is considered to be generic, it is illustrated by the production of green hydrogen from renewable sources. In order to ensure the operating safety and energy efficiency of the system, the objective is to maximize the life duration of the electrolyzer and the batteries by avoiding excessive stored quantities. Simulations using data obtained from a laboratory platform which replicates the process at a smaller scale highlight the effectiveness of the proposed approach.

Keywords: Operating Modes Management; Hybrid-Driven; Remaining Useful Lifetime; Optimization; Degradation Capacity; Green Hydrogen Production Stations

1. Introduction

From a general point of view, an industrial system is designed to fulfill several missions. The missions associated with a green energy production system, for example, aim to guarantee the availability of energy, while ensuring the safety of the system, the environment, and users. These missions are based on the services provided by the components that make up the system. For example, the mission to deliver energy, provided by the green energy production system, requires an energy harvesting service and an energy storage service. In turn, each sub-service calls on other lower-level services, such as transforming solar energy into electrical energy, and so on, according to a top-down functional decomposition. The highest level of this decomposition corresponds to the missions performed by the system itself, and the lowest level corresponds to the elementary services provided by the elementary components making up the system [1].

To avoid the situation where a service can no longer be performed when a hardware resource fails or when input data is unavailable, several versions can be implemented to perform the same service [2]. The surplus energy produced by a photovoltaic (PV) panel, for example, can be stored in electrical form in a battery, or as hydrogen form via an electrolyzer. Another example is the use of a wind turbine as an alternative solution to the PV panel when there is insufficient sunlight. Each version is characterized by a distinct set of hardware resources and consumed

data. Versions are ordered by the designer according to criteria such as reliability, precision, and safety. In a non-faulty situation, the nominal version of the service, i.e. the version with the highest level in the order of preference, is executed. In a faulty situation, the eligibility of each degraded version is evaluated according to the predefined order of preference [3]. If no version can be executed, the service becomes unavailable. The existence of these multiple versions increases the resilience of the system to hardware failures and external disturbances. A failure occurs when a component or group of components can no longer perform its function [4]. It manifests itself through a number of effects, called defects, faults, or symptoms, corresponding to a discrepancy between the actual value of a physical quantity and the value predicted by a normal behavior model. Evaluating the availability of a service requires two types of algorithms. The first type involves Fault Detection and Isolation (FDI) algorithms, which detect the discrepancy between the observed behavior and the predicted behavior, and can possibly identify the erroneous data [5]. The second type encompasses diagnostic algorithms, which enable the origin of the fault to be traced, the availability of the hardware resources used to provide the service to be assessed, and the list of services provided by each component to be updated [3, 6–8]. It can even lead to the introduction of backup components to fulfil the services when a fault occurs [9].

According to the phase of the life in which it is used and the external conditions of its use, a component, whatever its level of decomposition, has one or more well-defined objectives to achieve. An electrolyzer, for example, can only start producing hydrogen (production phase) once its internal pressure has reached a certain value (preparation phase). In the same way that a software application is decomposed into coherent menus, the set of services provided by a component is structured into Operating Modes (OM) [2, 4]. Each OM groups the services required to achieve the OM objectives. The conditions for switching from one mode to another are clearly defined. They are based on the evaluation of the values of the system inputs, the values of the desired system outputs, the state of the system represented by inner variables, and the results of the FDI and diagnosis algorithms. A hybrid automaton is commonly used to manage the different OM and their transitions. It allows encompassing the discrete behavior of the system linked to the switching between OM and the continuous part where, within a mode, the state variables, modified by the execution of the services belonging to the mode, follow a continuous temporal evolution [10]. Transitions of this automaton are classically triggered by Boolean functions of Boolean variables [11]. The Boolean variables involved in these transitions are themselves obtained, more or less directly, from the measured output and the users' system operating requirements. The OM management is considered to be event-driven since it relies on instantaneous data. For a renewable energy system, examples of events are (i) the wind speed being higher than a predefined threshold, and in this case, the wind turbine must be stopped for safety reasons, (ii) the state of charge of the battery indicating that this last is full, (iii) the required production is between two predefined values, and so on.

The new idea developed in this paper is to define mode change conditions not only based on real-time data but also based on predictive data, using OM formalism. The used predictive data are relative to the system operating conditions. These include quantitative estimates of the input and output flows of the system, in other words, the data that are consumed and produced by the system. From these predictive data, a predictive temporal sequence of OM changes can be defined by an optimization algorithm. The new idea is to add the remaining useful lifetime of the components as a constraint for the optimization algorithm, to the existing constraints relating to system reliability and safety. It is known, for example, that too frequent switching, or an excessive rate of use, can accelerate the degradation of a component. The final goal, is to maximize the operational lifespan of the system and reduce its overall operating cost by selecting appropriately the switching times. The proposed method and the corresponding optimization algorithm are a way of managing dynamically the preferred order of the different versions which was previously defined once and for all at the system design stage. Therefore, the operating mode management (OMM), as it leans on a predictive time temporal sequence and real-time events, becomes a Hybrid-Driven Operating Mode Management, hence extending the Event-driven method developed in [9]. One of the main difficulties is to formalize the optimization problem corresponding to the management of switchings between the operating modes.

The remainder is structured as follows. In Section 2 the Green Hydrogen Production Station (GHPS) is used to illustrate the theoretical notions that are developed all along the paper. In Section 3, a hybrid dynamical model to represent the continuous and discrete parts of a hybrid dynamical system structured into OM is proposed. The new concept of Hybrid-Driven Operating Mode Management is then presented. Its advantages, compared with those of the Event-Driven method, are highlighted. Section 4 defines the optimization problem and its constraints, first in

a general form and then applied to the specific case of the GHPS. Section 5 gives and analyses the obtained results. Section 6 provides the conclusions.

2. Green Hydrogen Production Station

The Green Hydrogen Production Station (GHPS) presented in **Figure 1** serves as an application to illustrate the scientific contributions developed in this paper. GHPSs are an answer to climate change and the necessity to develop solutions to produce clean energy. Indeed, the current ecological transition requires the maximum exploitation of renewable energies. However, unlike generation of hydrogen using nuclear power [12], the disadvantage of some sources such as solar and wind is their intermittency. In order to guarantee a given level of service, it is therefore necessary to store the surplus production and release it when the production conditions no longer cover consumption needs [13]. As a GHPS is built from multiple components presenting different OM, that need to be managed according to the production conditions and the safety measures, it can be considered as a Hybrid Dynamical System. The behavior of a GHPS evolves continuously with respect to the time inside an OM and discontinuously during the OM switching, because of the numerous multi-operating mode possibilities between the variety of sources and storage units. Moreover, one of the biggest impediments to green hydrogen dissemination, aside the cost of the electrolyzer, is its lifetime that depend on materials, but also operation modes, (starts and stops, cycling, etc.) [14]. Morever, ref. [15] shows the influence of the capacity loss of the components, due to degradation, on the overall performance, and demonstrates that it can be critical. Hence, this paper focuses on the issue of extending equipment lifespan by employing optimal management of operating modes.

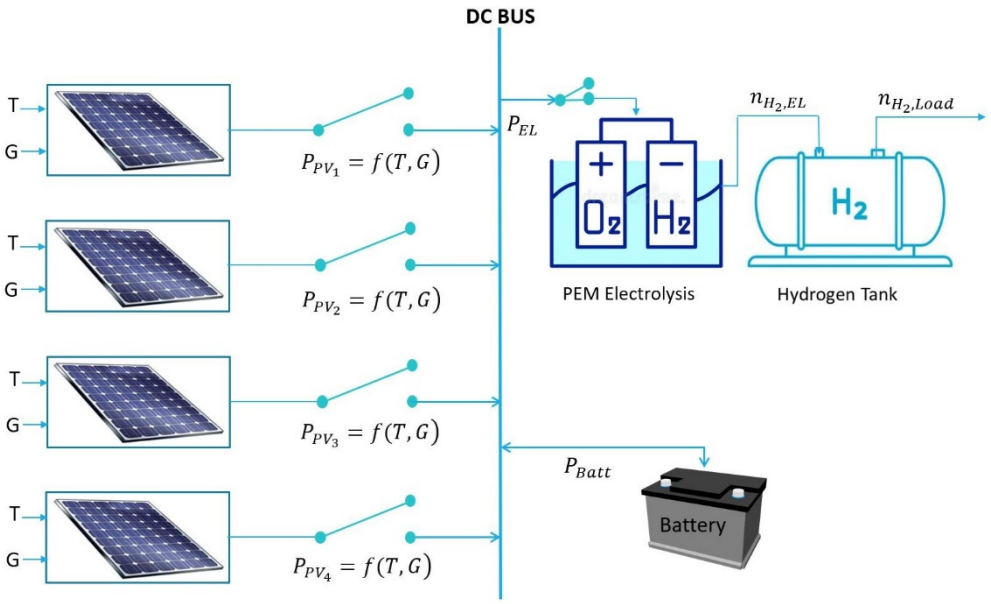

Figure 1. Green Hydrogen Production Station.

The proposed standalone GHPS, shown in **Figure 1** includes four photovoltaic panels (PV), a battery (Batt), an electrolyzer (EL), and a storage tank. These components may all be connected or disconnected to a DC bus. Only PV panels are used as renewable sources to facilitate the expression of future mathematical optimization problems. The PV panels have all the same characteristics and produce the same power P_{PVi} if they are submitted to the same solar irradiation G and temperature T. The potential surplus of energy produced by the PV can be stored in the form of hydrogen via the electrolyzer or in the form of electricity via the battery. Note that the battery not only plays the role of an energy storage element but is also required to maintain a constant power input to the electrolyzer since the latter cannot physically follow a renewable electricity production profile. In what follows, P_{EL} denotes the power at the input of the electrolyzer. $n_{H2,EL}$ is the quantity of hydrogen generated by the electrolyzer, $n_{H2,Load}$ is the quantity of hydrogen required by the user. P_{Batt} is the power at the input or the output of the battery (according to its positive or negative sign).

3. Operating Mode Management

3.1. Hybrid Dynamical System Modeling

Hybrid Dynamical Systems (HDS) represent a multifaceted class of mathematical models that find wide applications in various domains, including engineering, economics, biology, and control theory [10]. Depending on the nature of the discrete phenomena that govern them, several subcategories of HDS exist, among which are the jump linear systems, the mixed logical dynamical systems, and the switching systems. HDS studied here change from one discrete state to another when a Boolean condition is verified. They therefore belong to the class of switching systems [11, 16]. Many representations exist to describe the behavior of a switching system such as the Hybrid Neural Network, the Hybrid Bond Graph, and the hybrid automaton [10, 11, 16, 17]. As the optimization problem that will be exposed in the following requires a mathematical formulation of the continuous part of HDS, a modeling based on the hybrid automaton is chosen (Equation (1)).

It is defined by the structure *SS = (A, S, H),* where *A* is a deterministic automaton,

$$A = (M, T, OM_0) \tag{1}$$

A includes a finite set of discrete states or operating modes, $M = \{OM_0, OM_1,..., OM_m\} = \{OM_i, i \in I^m\}$. Each OM corresponds to a state (vertex) of the automaton. $T = \{t_{ij},(i,j) \in I^m\}$ describes a set of transitions, each of which is defined by $t_{ij} = \{OM_i, OM_j, c_{ij}\}$, where OM_i is the origin mode, OM_j is the destination mode, and c_{ij} symbolizes the firing condition. OM_0 is the initial mode where the system is located, the first time it is put into service.

$S = \{s_i, i \in I^m\}$ is a set of continuous models, describing the time evolution of the system in each mode (Equation (2)):

$$s_i = \begin{cases} \dot{x} = f_i(x, u, w) \\ y = h_i(x, u, w) \end{cases} \tag{2}$$

where $x = \{x_1, \cdots x_n\} \epsilon \mathbb{R}^n$ designs the continuous state space, $u = \{u_1, \cdots u_p\} \epsilon \mathbb{R}^p$ represents the continuous controllable inputs, $w = \{w_1, \cdots w_l\} \epsilon \mathbb{R}^l$ represents the continuous uncontrollable inputs, $y = \{y_1, \cdots y_q\} \epsilon \mathbb{R}^q$ corresponds to the system outputs. $f_i \epsilon \{f_1, \cdots f_m\}$ and $h_i \epsilon \{h_1, \cdots h_m\}$ represent a set of vector fields defining the continuous dynamics of the system.

H is a hybrid bijective map that associates a continuous model to each OM, defined in Equation (3):

$$\begin{gathered} H : M \to S \\ OM_i \to s_i \end{gathered} \tag{3}$$

in which each $OM_i \in M$ is associated to a model $s_i \in S$. In addition, $Init(OM_i)$, defined in Equation (4), defines the value of the vector *x* appearing in s_i, when the system reaches for the first time the mode OM_i.

$$Init(OM_i) : OM_i \to x^0 = \{x_1^0 \cdots x_n^0\} \tag{4}$$

The domain mode $D(OM_i)$ specifies the limits of the variables, as shown in Equation (5):

$$D(OM_i) : OM_i \to \{x^{inf}, x^{sup}\} \tag{5}$$

where $x^{inf} = \{x_1^{inf} \cdots x_n^{inf}\}$ and $x^{sup} = \{x_1^{sup} \cdots x_n^{sup}\}$ represent respectively the minimal and maximal values that the state variables can take when the system is in the OM_i operating mode. The system stays in OM_i while the values of the state variables remain in $D(OM_i)$ and switches to OM_j when the state variables enter domain $D(OM_j)$.

3.2. Operating Mode Management

An operating mode refers to a discrete state where the system operates according to a specific set of objectives using a specific subset of elementary components. Elementary components which are not in use are in the OFF mode.

Let $C = \{c_1, \cdots c_n\}$ be the set of the elementary components of the system *S* (*n* is the number of components). Let $M(c_i) = \{OM_1(c_i) \cdots OM_j(c_i)\}$ be the set of the operating modes of component $c_i \in C$ (*j* is the number of operating modes for the component c_i). The parallel composition of the operating modes of the elementary components

displays all the theoretical possible modes of the system *S*. Each one is represented by a vector:, defined in equation (6)

$$OM_i(S) = \{OM_i(c_1) \cdots OM_i(c_n)\} \tag{6}$$

named system mode and noted β in the following. However, some of them will never be reached as they do not have a meaningful purpose. Let $M(S)$ denote the set of possible OM for the system *S*. Two primary design paradigms for OMM control systems exist, which are Event-Driven and Time-Driven. First, the Event-Driven design paradigm is characterized by its capacity to respond to events in real-time, which makes it ideal for managing with asynchronous external stimulation. Indeed, an Event-Driven OMM reacts each time the occurrence of a new event is detected. Events are related to uncontrolled inputs that exceed threshold values, to deliberate human actions (user requirements), or to the occurrence of faults (State of Health). This is only at the time of the event occurrences, that the system mode β can be modified (see **Figure 2**). The operating mode for each elementary component is then updated. Faulty components are turned to safe or OFF mode. This corresponds to the management of the discrete part of the system. Once the OM of the elementary components is determined, control signals to bring the system into the desired state can be generated using the continuous models s_i (Equation (2)) associated with each mode OM_i[18, 19].

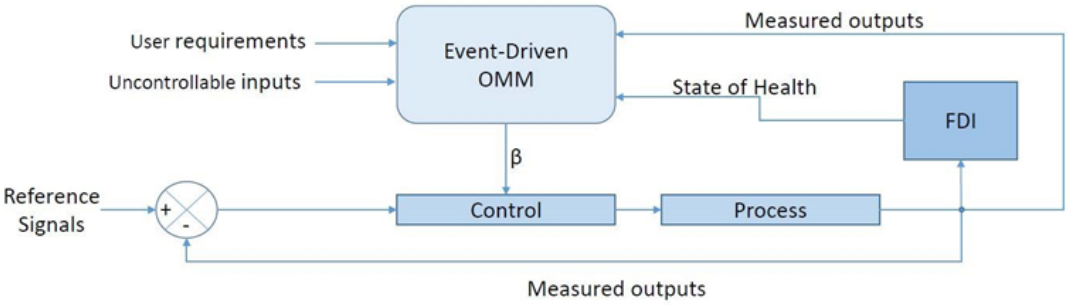

Figure 2. OMM Event-Driven Systems.

The Time-Driven design paradigm, on the other hand, is more like a predictive approach. The temporal evolution of the data consumed and produced by the system is assumed to be more or less known in advance. It then becomes possible to determine in advance the instants at which the OM switching must be performed so that the system follows the pre-defined trajectories. Instead of being a system reacting to asynchronous events whose arrival times are totally unknown, the system becomes a time-driven system since its evolution can be totally planned. The temporal and synchronous properties of a time-driven model serve to ensure a deterministic and predictable behavior. Manufacturing processes where objectives of production are well defined in advance or scheduling systems for public transportation are examples for which the Time-Driven OM is a convenient approach.

To achieve efficient system performance, a Hybrid-Driven approach to govern the OM of a Hybrid Dynamical System is proposed in this paper. Indeed, the behaviour of a system is never totally predictable or unknown. The missions that the system must fulfill, the environmental conditions in which it operates, and the expected performances are defined in the specifications that precede its realization. This defines the predictable side. The indeterminate side is linked to hardware failures or external disturbances such as a change in production targets or environmental conditions.

Figure 3 summarizes the principle of a Hybrid-Driven OMM. Using predictive system inputs and outputs, given on time windows of length *H*, the temporal sequence:

$$\beta_H = \left\{\beta_{t_1}, \cdots \beta_{t_i}, \cdots \beta_{t_p}\right\} \; with \; t_i \in [t_0 \cdots t_0 + H] \tag{7}$$

of the system modes, that maximizes the pre-defined system Key Performance Indicators (KPI) is elaborated by the Time-Driven part of the OMM. This optimal temporal sequence is then used as an input by the Event-Driven part to be adjusted according to the value of the real data and the unpredictable asynchronous events.

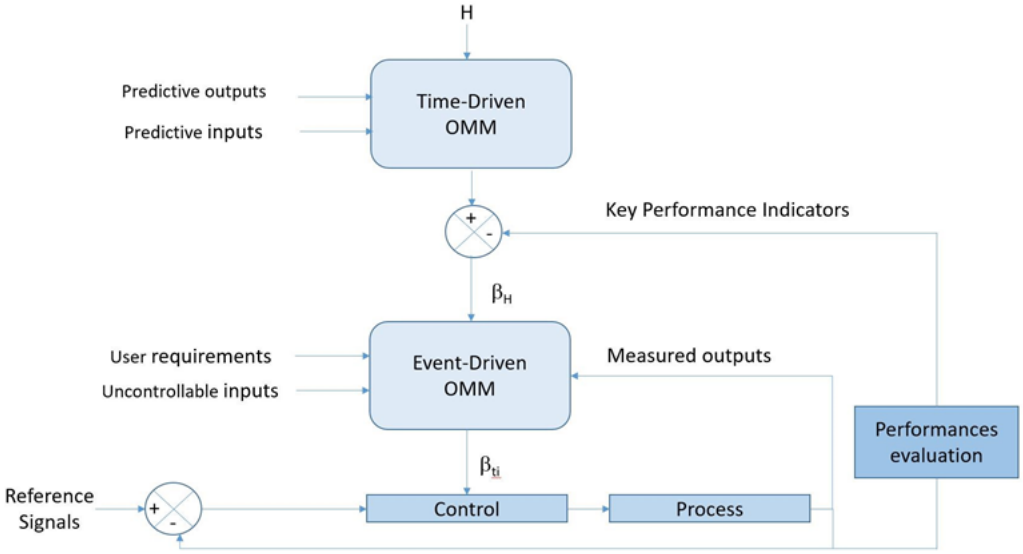

Figure 3. Hybrid-Driven OMM of a GHPS hydrogen.

More precisely, in Equation (7), t_i represents a time where an OM switching occurs and β_{ti} is the value of β at time t_i. That means that β_{t_i} is different from β_{ti-1} and from β_{ti+1}. Assume now, that at the time $t \in [t_{i-1}, t_i]$, the system operates according to the mode defined by β_{ti-1}, the Event-Driven part checks that all the conditions defined by the energy and safety constraints are satisfied for the system to work at time t_i in the mode defined by β_{ti}.

3.3. Application to the Green Hydrogen Production System

In the specific case of the system described in **Figure 1**, elementary components are of 3 types: Photovoltaic Panels, electrolyzer, and battery. Each of them displays several OM. The complete OMM automaton for the EL is given by **Figure 4**. Starting from the OFF mode and receiving a Start of use signal (external event), the EL goes through a pressurization step until the internal pressure $pres_{H2}$ value reaches a predefined value (inner event). The EL is then in the Standby OM until it receives an order for production, and so on.

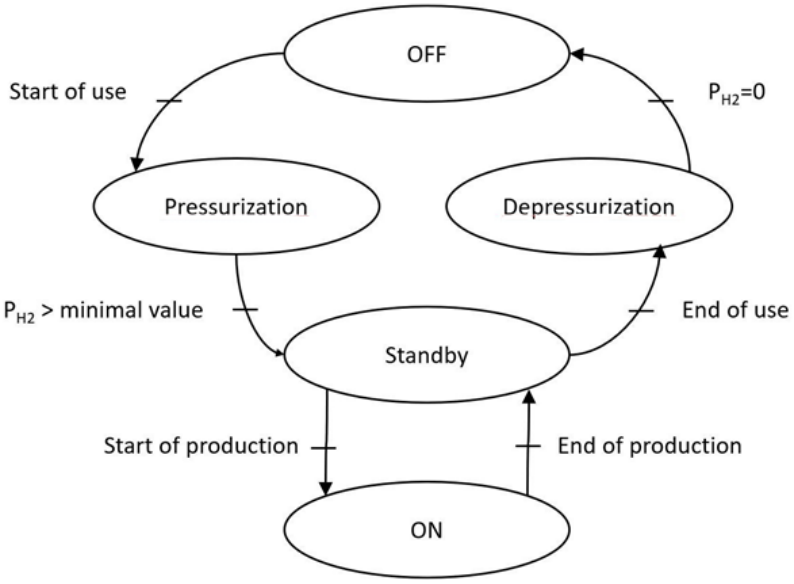

Figure 4. OM automaton for the electrolyzer.

In the remainder of the paper, the GHPS is assumed to be in the production mode. That means that only a subpart of the OM of the elementary components is considered. They are listed as follows with their associated missions.

- $OM(PV)$ = {*ON, OFF*}. In the OFF mode, the PV is disconnected from the DC bus and its mission is not to generate electricity (P_{PV} = 0). In the ON mode, the PV is connected to the DC bus and its mission is to produce $P_{PV} = f(T,G)$ as defined by the continuous behaviour model associated with this OM.
- $OM(EL)$ = {*Standby, ON*}. In the production OM of the system, the EL is assumed to be under the required pressure to produce hydrogen. In the Standby OM, the associated mission is not to produce hydrogen ($n_{H2,EL}$ = 0). In the ON mode, the mission is to generate $n_{H2,EL} = f(P_{EL})$ (cf. **Figure 1**).
- $OM(Batt)$ = {*Charge, Discharge*}. The battery is always connected to the DC bus. It is required to maintain a quite stable power at the input of the EL. In the Charge OM, the mission is to increase the battery state of charge (SOC). In the Discharge OM, the mission is to use a part of the stored charge, and the SOC value consequently decreases.

3.3.1. Event-Driven OMM

Using the services provided by these elementary components the system missions, in the production mode, can be fulfilled. In the case of an Event-Driven OMM, these consist essentially of ensuring the energetic balance, guaranteeing there is no disruption in the energy supply for the final users, and maintaining the safety of the system [13]. In the paper [13] a basic Bond-Graph multiphysics modelling of a power cell with an electrolyzer, based on power flows in the system, is given, and extended later in [20, 21] for diagnosis purposes. The Event-Driven OMM introduced in [13] is a one step ahead algorithm, depending on an event (e.g., sudden change of solar power, change in the load) whereas the current paper deals about predictive management based on weather or load predictions. The results are, indeed, fundamentally different, and, in the case study, the EV OMM could let the number of solar panels constant (if no change is triggered).

As represented by **Figure 5**, the Event Driven OMM consists in determining the global system OM β_{ti} = (OM(PV_1), OM(PV_2), OM(PV_3), OM(PV_4), OM(Batt), OM(EL)) according to:

- The instantaneous multi-sources harvesting capability, represented by $P_{PV} = PPV_1 + PPV_2 + PPV_3 + PPV_4$.
- The instantaneous energy request, represented by $n_{H2,Load}$.
- The instantaneous quantity of energy stored in the battery and in the hydrogen tank, represented respectively, by the state of charge *SOC* of the battery and the pressure $pres_{H2}$ in the hydrogen tank.
- The state of health (*SoH*) given by FDI algorithms.

As previously said, once the system OM is determined, control algorithms are used to give the system outputs the values defined by the reference signals.

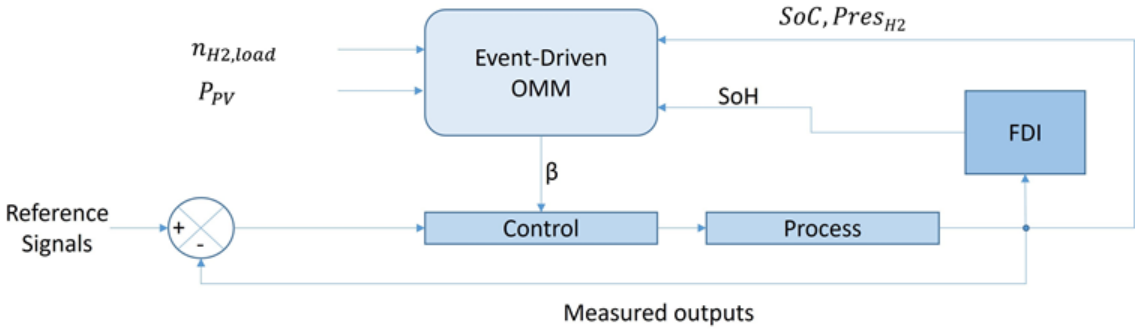

Figure 5. Event-Driven OMM of the GHPS.

3.3.2. Hybrid-Driven OMM

For a such system as the considered GHPS, profiles of the energy to produce and of the collectible energy, on a given time horizon, can be obtained from historical real-time data of consummation and weather forecasts.

The original idea developed in this paper is then, to use these predictable data to generate the optimal sequence of OM switching to ensure the previously defined system objectives (energy efficiency, system safety) while minimizing the system degradation. Indeed, switching between the different OM too often, or staying in a mode for a too long time, can shorten the lifespan of a component and consequently increase the overall system operating cost.

As explained by **Figure 6**, using predictive power data of the sources $\hat{P}_{PV}$ and predictive load $\hat{n}_{H2,Load}$ given on the time horizon H, the OMM Time-driven part of the Hybrid-Driven OMM generates the optimal sequence of system mode switching which maximizes the KPI. The lifetime of the storage components (battery and electrolyzer), which can be thought of as the most expensive system devices, is included in these KPIs. The Remaining Useful Life (RUL) of these components is estimated in real-time from the performance evaluation algorithms, including FDI and prognosis [11, 22] and compared to a reference frame. The Event-Driven OMM receives the optimal OM switching sequence β_H and checks using the real instantaneous data $n_{H2,load}$, P_{PV} and the detected faults that the next predictive system OM β_{ti+1} is consistent with the actual system behaviour. Note that faults are not taken into account in the following.

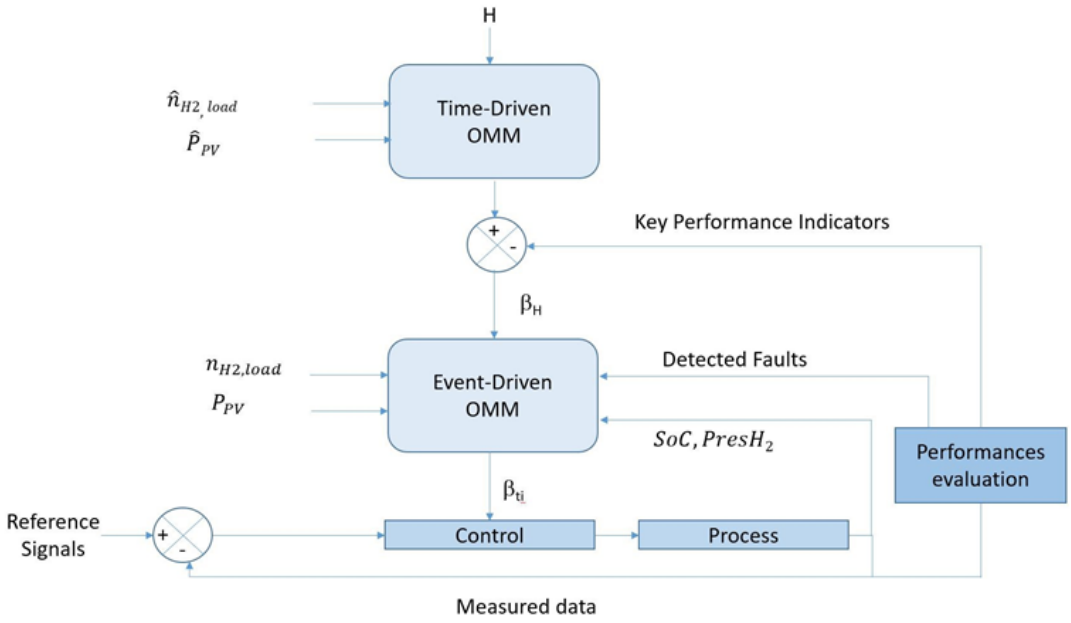

Figure 6. Hybrid-Driven OMM of the GHPS.

4. Optimal Hybrid-Driven Operating Mode Management

4.1. Predictive Optimization Problem Formulation

A standard optimization problem can be defined in Equation (8):

$$\begin{gathered} J = \min f(x) \\ x \in \mathbb{X} \\ \text{subject to } S = \{x \in \mathrm{X} : h(x) = 0, g(x) \leq 0, lb \leq x \leq ub\} \end{gathered} \tag{8}$$

where the decision variables that can be controlled are represented by the symbol x and where $\mathbb{X}$ is their feasible region space. The equality constraints are represented by the function h, while the inequality constraints are defined by the function g. lb and ub represent the lower and upper bounds of x respectively. For a switching system defined by the structure given by Equation (1), the decision variables are the operating modes OM_i and the control

inputs u of continuous models s_i associated with each OM_i (Equation (2)).

In the case where the objective is to extend the remaining lifetime of a system, i.e., to minimize the degradation of each of its fragile components, the optimization problem becomes a multi-objective optimization problem (MOOP) [23]. Several approaches exist for simplifying a MOOP into a single-objective problem, e.g., [24]. The Weight Sum Method (WSM), which allows the transformation of a MOOP to a linear weighted sum of various objectives is well known [25, 26] and chosen in this case. The weight of an objective is given based on its importance compared to other objectives. The optimization problem, in Equation (9) becomes:

$$J = \min F(x) = \min_{x \in \mathbb{X}} \langle f_1 \cdots f_M \rangle = \sum_{i=1}^{M} \rho_i f_i \tag{9}$$

where $\sum_{i=1}^{M} \rho_i = 1$, $\rho_i \geq 0$, $F(.)$ represents the total degradation of the system and $f_i(.)$ the degradation of the component c_i.

4.2. Application to the Green Hydrogen Production System

In the case of GHPS which serves as an application to illustrate the proposed approach, the degradation of both the battery and the electrolyzer are considered.

Several factors affect the lifetime of a battery, among them the number of partial cycles, the current flow, the cell voltage, the depth of charge-discharge cycles [27–29].

The following formula, Equation (10), proposed by Schiffer [30] is used to compute the degradation capacity $C_{deg,Batt}$ of a battery:

$$C_{deg,batt}(t) = C_{deg,limit} e^{-c_x\left(1-\frac{Z_W(t)}{1.62 Z_{IEC}}\right)} \tag{10}$$

where $C_{deg,limit}$ is the degradation capacity at the end of the life (i.e., 80% of the nominal capacity), Z_{IEC} is the number of charge-discharge cycles fixed by the International Electro-technical Commission (IEC) at which the battery is considered to have a remaining capacity of 80% compared to its nominal capacity (given by the datasheet), c_z represents a constant parameter equivalent to 5 and where $Z_W(t)$ is given by Equation (11):

$$Z_W(t) = \frac{1}{C_N} \int_0^t I_{dch}(\tau) f_{SOC}(\tau) f_{acid}(\tau) d\tau \tag{11}$$

In Equation (11), C_N is the nominal capacity of the battery, I_{dch} is the current of discharge, f_{acid} denotes the impact of acid stratification, it would be considered as constant, and f_{SOC} is a weighted sum of three degradation parameters, which are [31]:

1. The amount of bad recharges. This might have an impact on active mass degradation. A recharge is considered unsuccessful if the value of *SOC* attained at the end of a filling exceeds the value of the completely charged state ($SOC > SOC_{limit}$).
2. The time since the previous full recharge. Indeed, to increase battery life, regular full battery recharges are required.
3. The minimum value of *SOC* since the last full recharge. When the value of *SOC* of the battery since its recent full recharge approaches zero, the concentration of acid stratification rises, causing the electrolyte to deteriorate.

Degradation models of electrolyzers are more difficult to obtain, because of the complexity both of the system and complicated phenomena including chemical reactions with materials and impurities [32]. In the literature, lifetime (in particular for electrolyzers) are estimated from statistical methods using real data provided by users (e.g., MTBF) [3]. Finally, the lifetime of an equipment can be estimated from the different components, using reliability models such as fault-tree analysis. Another promising method relies on data and prediction with machine learning methods, but it requires a lot of experimental data for training [33]. Experimental studies, in general, are done with steady operating conditions, or accelerated stress tests that do not correspond to the operation of EL powered by renewables. Therefore, it is barely impossible to perform comparison with existing degradation studies, and the aforementioned methods cannot be applied directly to the presented system because of the lack of data.

There are very few model based estimates of electrolyzers State of Health, the most complete being supplied in [34] , which, however, should be calibrated by the concentration in ferrous ions of water, generally unknown, and does not take start-stops into account which are of importance as demonstrated only qualitatively in [35].

As shown by Equation (12), it is proposed to calculate $C_{deg,EL}(t)$ by taking into account the cumulative production times and the number of switching between the EL modes.

$$C_{deg,EL}(t) = C_{deg,EL}(t_{i-1}) + \alpha_1 OM_{t_i}(EL) + \alpha_2 \left(OM_{t_i}(EL) - OM_{t_i-1}(EL)\right) \tag{12}$$

where α_1 and α_2 are two constants ($\alpha_1 \leq \alpha_2$), OM_{t_i-1} is a binary representing the mode of the EL at the previous switching time t_{i-1} and $OM_{t_i}(EL)$ describes the new mode of at time t_i. It is computed as proposed by Equation (13).

$$OM(EL) = \begin{cases} 0 & if\ electrolyzer\ is\ on\ Standby\ mode \\ 1 & if\ electrolyzer\ is\ ON \end{cases} \tag{13}$$

Using these degradation models, the optimization problem can now be formulated. Over a time window H, it predicts the optimal times for the mode changes and the value of the modes that minimize the total system degradation. It is expressed by Equation (14).

$$\begin{matrix} \min C_{deg,Tot} \\ \beta \in \mathbb{M}(S) \end{matrix} \tag{14}$$

where $C_{deg,Tot} = w_1 C_{deg,batt}(H) + (1 - w_1) C_{deg,EL}(H)$, subjected to constraints given by relations from Equation (15) to Equation (21).

The energy balance equation is:

$$n_{PV}\hat{P}_{PV}(t) + P_{battref}(t) - P_{EL}(t) = 0 \tag{15}$$

The value $\hat{P}_{PV}(t)$ represents the PV predictive power. It is obtained from the weather forecast. P_{EL} represents the power of the electrolyzer. It can be calculated from the EL datasheet as shown by Equation (16):

$$P_{EL} = \begin{cases} P_{EL,Standby} & \text{if electrolyzer is on Standby mode} \\ P_{EL,ON} & \text{if electrolyzer is ON} \end{cases} \tag{16}$$

$P_{Battref}(t)$ is fixed by the PI controller that controls the input current I_{Batt} at each time [36].

Batteries manufacturers generally specify two variables in the data sheet of the battery: $I_{Batt}^{C,max}$ and $I_{Batt}^{d,max}$, which represent the maximum battery charging and discharging currents respectively. These two values entail constraints given by Equation (17).

$$\begin{matrix} I_{Batt}(t) \leq I_{Batt}^{C,max} \text{ while the battery is being recharged} \\ I_{Batt}(t) \leq I_{Batt}^{d,max} \text{ while the battery is being discharged} \end{matrix} \tag{17}$$

Constraints are given by Equation (18) state that there must be a minimum time between two mode changes for the PV and EL. Too frequent switching could damage these components. $OM_{ti-1}$is the OM at t_{i-1}, OM_{ti} is the OM at t_i and $\Delta T_{min,.}$ is the minimal time between two switchings.

$$\begin{matrix} t_{i-1}\left(OM_{t_{i-1}}(PV_x)\right) + \Delta T_{min,PV_x} \leq t_i\left(OM_{t_i}(PV_x)\right) \\ t_{i-1}\left(OM_{t_{i-1}}(EL)\right) + \Delta T_{min,EL} \leq t_i\left(OM_{t_i}(EL)\right) \end{matrix} \tag{18}$$

Note that determining the modes of each PV is equivalent to determining the number of PV electrically connected to a DC bus. Therefore, the constraint given by Equation (19) expresses that the number of PV n_{PV} that can be connected to the DC bus is between *lb* and *ub*.

$$lb \leq n_{PV} \leq ub \tag{19}$$

Constraints given by Equation (20) and Equation (21) express the physical limitations enforced by storage components. *SOC* limits and pressure in the hydrogen storage tank $pres_{H2}$are considered.

$$SOC_{\min,limit} \leq SOC \leq SOC_{\max,limit} \tag{20}$$

$$\text{pres}_{\text{H2,min}} \leq \text{pres}_{\text{H2}} \leq \text{pres}_{\text{H2,max}} \tag{21}$$

The optimization problem can therefore be formulated with a finite number of variables n_v, given by Equation (22):

$$n_v \leq \frac{H}{\Delta T_{min,PV_x}} u_b + \frac{H}{\Delta T_{min,EL}} \tag{22}$$

As the optimization program is non-convex and involves integer/binary variables, it is solved using a genetic algorithm [37], provided by the Matlab/Simulink software.

5. Results and Discussion

The numerical values used for the simulation are collected from the platform located in Laboratory *CRIStAL* at Ecole Polytechnique Lille, which replicates a real system on a smaller scale [32]. The PV profile was collected from actual values (**Figure 7a**), and the electrolyzer demand side was consistent with the hydrogen output.

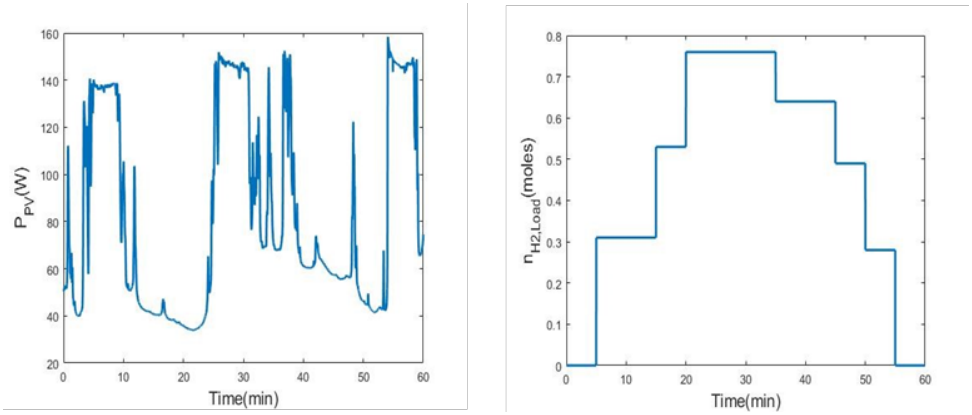

(**a**) (**b**)

Figure 7. Predictive renewable power and hydrogen demand. (**a**) Predictive power produced by one PV; (**b**) Predictive quantity of demanded hydrogen.

The number of PV panels is n_{PV}= 4. All of them have equal production power when they are turned on. The electrolyzer has a rated power of $P_{EL,ON}$= 300 W and a standby power of $P_{EL,Standby}$= 70 W. When turned on, it produces hydrogen at a flow rate of $n_{H2,rated}$= 0.6 moles/hour at 11 bar. The hydrogen tank has a storage capacity of V = 0.015 m^3, and the operating pressure ranges from a minimum of $pres_{H2,min}$= 1.5 bar to a maximum of $pres_{H2,max}$= 11 bar. The tank operates at a temperature of T = 333 K. The nominal capacity of the battery is C_N= 100 Ah. To avoid assuming an ideal scenario where the initial SOC is set to 1, the initial SOC of the battery is set to 0.6. The weight assigned to the battery degradation (w_1) is 0.3, while the weight assigned to the electrolyzer degradation ($1 - w_1$) is 0.7. This is because the cost of replacing or repairing the electrolyzer due to degradation is higher than the cost of addressing the degradation of the battery. The length of the time window H is equal to 60 minutes. The minimal time between two switchings is $\Delta T_{min,.}$= 15 min for both the EL and the PV. To demonstrate the relevance of the proposed approach, Hybrid-Driven OMM and Event-Driven OMM are compared. For both methods, the same characteristics and input data are used. In event-driven OMM, n_{PV} remains constant and equals two during the time window H. **Figure 7a** and **b** depict the predictive power generated by a single PV panel $\hat{P}_{PV}$ and the expected amount of hydrogen required by final user $\hat{n}_{H2,Load}$ over time, respectively. Based on the simulation results of the Hybrid-driven OMM, it can be shown in **Figure 8a** that EL is turned ON at t = 5 min, coinciding with the start of hydrogen demand by the load, and it remains ON until t = 51 min even if the load continues to request hydrogen until t = 55 min. The power of the EL is directly proportional to the hydrogen demand. It is interesting to note that there is only one start and one stop for both strategies, but the hybrid driven is different because it aims, in general, at a better allocation of resources in order to minimize the degradation.

For the remaining 4 min, instead of keeping the EL ON, the hydrogen stored in the hydrogen tank can be utilized since the pressure at t = 51 min is 4.23 bar as it is shown in **Figure 9a**, which is above the minimum pressure

requirement of $pres_{H2,min}$. On the other hand, in the Event-driven OMM scenario, EL is turned ON at t = 5.5 min and remained ON until t = 59 min as illustrated by **Figure 8b**. EL does not switch to Standby mode before this time because the switching threshold in Event-driven OMM is determined by the limits set in Equation (18).

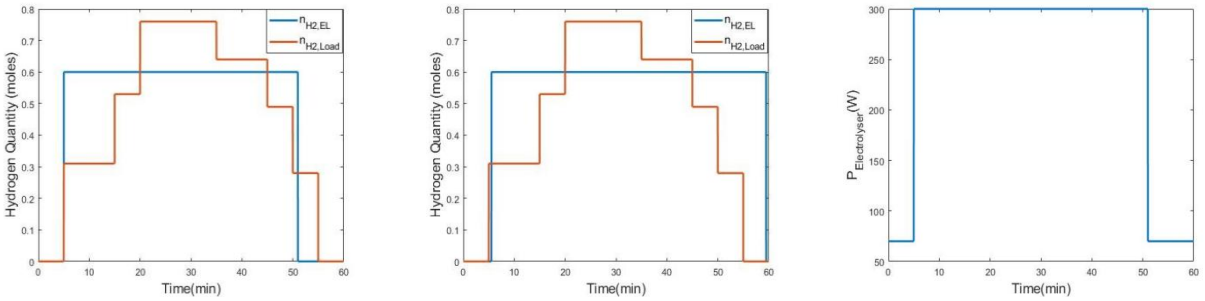

(**a**) (**b**) (**c**)

Figure 8. Comparison of hydrogen flows. (**a**) Produced and consumed n_{H2} in hybrid driven OMM; (**b**) and in event-driven OMM; (**c**) EL Power for hybrid driven.

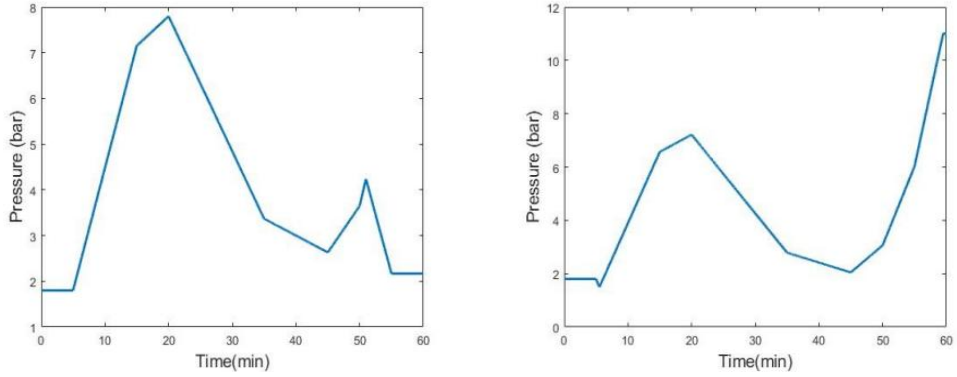

(**a**) (**b**)

Figure 9. Comparison of storage tank pressures. (**a**) Pressure in the storage tank, Hybrid-driven OMM; (**b**) and in event-driven OMM.

When the pressure of hydrogen in the hydrogen tank reaches a limit bound, EL switches modes. This behavior can be observed in **Figure 9b**, where the pressure of hydrogen in the hydrogen tank reaches 1.5 bar, causing EL to turn ON and remain ON until the pressure reaches the upper limit. **Figure 10a** gives the profile of n_{PV} determined by the genetic algorithm in the case of Hybrid-driven OMM. It can be shown that at t = 2 min, two PV panels were turned ON and remained active until t = 22 min when two additional PV panels were activated.

Comparing this profile with **Figure 7a**, it is obvious that there was a significant drop in P_{PV} to around 40 W per panel between t = 22 min and t = 24 min, which explains the subsequent increase in n_{PV} to 4. As the power output of a single PV panel increased over time, the value of n_{PV} changed accordingly. At t = 24 min, n_{PV} decreased to 3, and then to 2 at t = 26 min. From then on, n_{PV} remained constant until t = H, in compliance with Equations (18) and (19). When one PV panel was turned off at t = 24 min, the switch was executed using Equation (18) because the time interval Δt = 24 − 2 = 22 min was greater than the minimum time interval $\Delta t_{min,PVx}$= 15 min, and the number of PV panels turned off (in this case one PV is turned OFF) was lower than the n_{PV} that was ON at t = 2 min (n_{PV} = 2 at t = 2 min). The same process was applied to the second PV panel that was turned off at t = 26 min. In addition, the n_{PV} varied between the lower bound lb = 0 and the upper bound ub = 4 as specified in Equation (19).

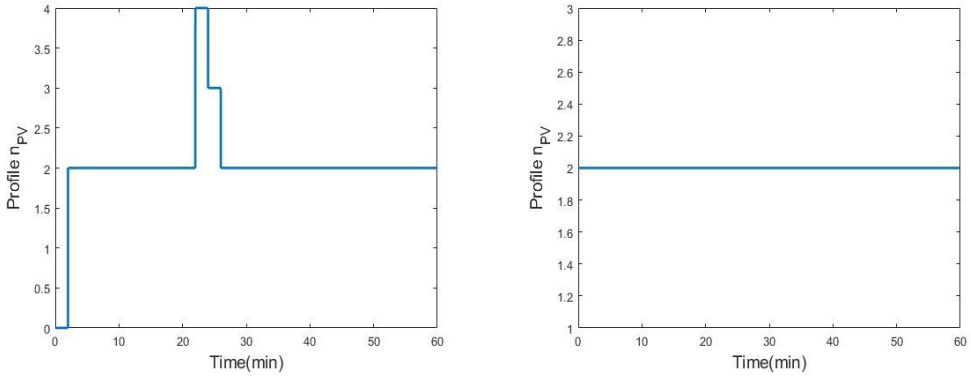

(**a**) (**b**)

Figure 10. Comparison of solar panel profiles. (**a**) Profile n_{PV} in Hybrid-driven OMM; (**b**) Profile n_{PV} in Event-driven OMM.

Figure 11 illustrates the global power generated by the PV panels connected to the system, along with the power requested by the electrolyzer over a time period of H in both scenarios. At times, the total power generated by the PV panels (n_{PV}×P_{PV}) may exceed the power produced by EL (P_{EL}). In such cases, the surplus energy is stored in the battery, increasing the SOC of the battery. Conversely, there may be times when the power generated by the PV panels is lower than P_{EL}, and in such cases, the battery can be utilized as a source of power to bridge the gap between n_{PV}× P_{PV} and P_{EL}. The SOC of the battery was observed to start at 0.6 in both scenarios and fluctuate over time as it is shown in **Figure 12**. SOC values were affected by surplus energy, which led to an increase, as well as by deficit energy scenarios or self-discharge, which caused a decrease.

To compare the results, **Table 1** displays the capacity degradation for the battery, electrolyzer, and total degradation capacity calculated using Equation (14). **Table 1** shows that at time t = H, the degradation capacity of both devices in Hybrid-driven OMM is lower than that in Event-driven OMM, indicating that the RUL of each device is maximized using hybrid-driven OMM. Therefore, the proposed method leads to a 14.35% improvement in the overall degradation of the system.

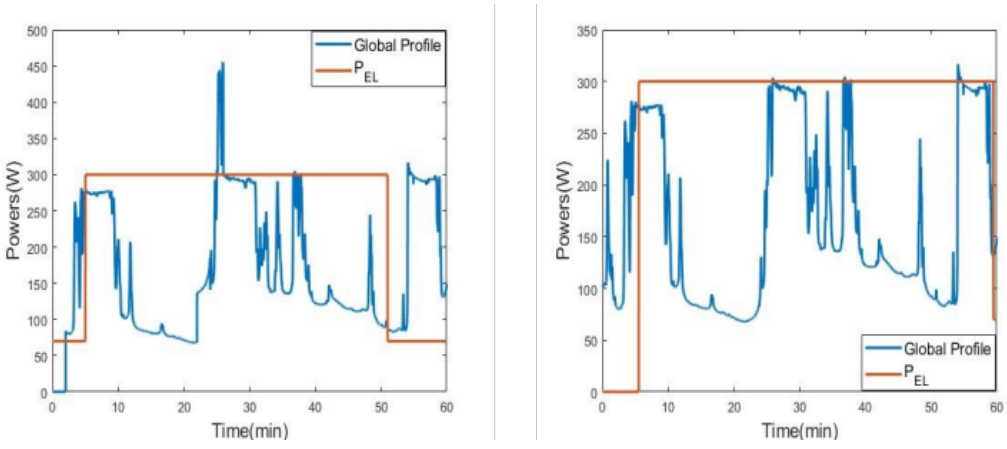

(**a**) (**b**)

Figure 11. Comparison of power profiles. (**a**) The global profile of powers in Hybrid driven OMM; (**b**) in event driven OMM.

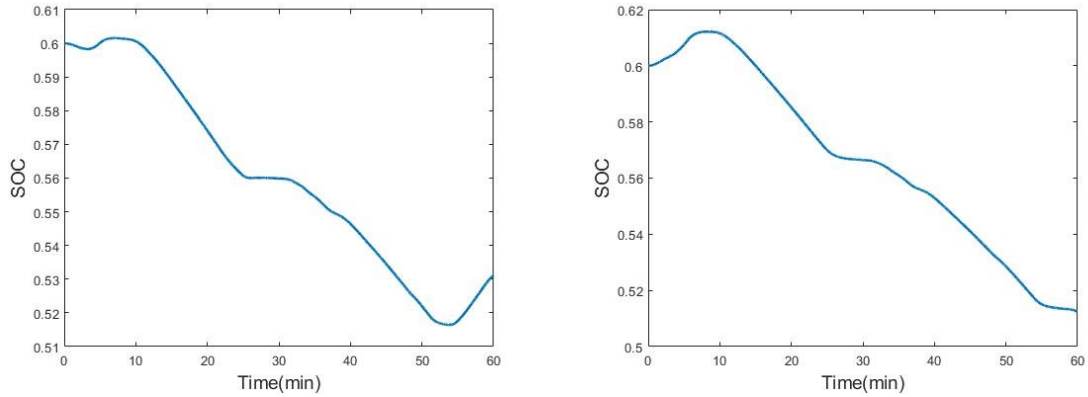

(**a**) (**b**)

Figure 12. Comparison of SOC. (**a**) SOC of the battery in Hybrid driven OMM; (**b**) and in Event-driven OMM.

Table 1. Comparing storage devices degradation capacity at t = H between Event-Driven and Hybrid-Driven OMM.

Capacity of Degradation	Event-Driven	Hybrid-Driven
$C_{deg,Batt}(H)$	0.1428	0.1423
$C_{deg,EL}(H)$	55.57	47.59
$C_{deg,Tot}(H)$	38.9419	33.35

The method itself proves that the lifetime of a system can be significantly extended by a Hybrid-Driven OM management rather than an Event-Driven one as it is conventionally implemented. Indeed, throughout the proposed application, a series of approximations have been done, ranging from the estimation of the EL degradation factor, to the selection of weight values (w_1, w_2, etc.), and finally to the choice of the $\Delta t_{min,PVx}$ and $\Delta t_{min,EL}$. These deliberations, though demanding, played a decisive role in shaping the final result. The main strength of the method is that it can be extended to more complicated systems with many different OM. One of the limitations of the study is that the inputs should be close to the predictions, which means that the method is valid for reasobaly short time windows. An extension would be to consider a stochastic prediction error, obtained from experiments, and compute service rates or probabilities of degradation level.

When closely looking at the degradation factors for hybrid driven OMM, in **Figure 13**, one can see that the EL profile is better balanced, there are also two starts and stops, but the duration of the stand-by phase is more important, which allows to extend the lifetime. Regarding the battery, the overall degradation is much smaller than that of the EL. The most important difference of degradation factor with the Event driven strategy, in this case, is mainly due to the evolution of the SOC_{min} which is marginally better as shown in **Figure 13b.**

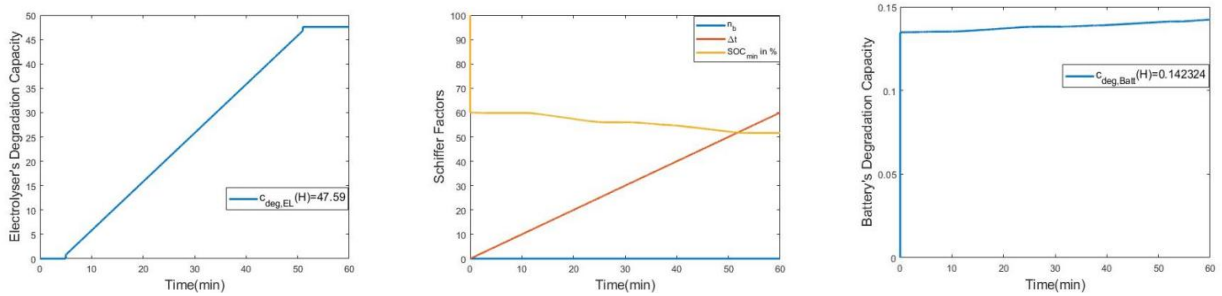

(**a**) (**b**) (**c**)

Figure 13. Hybrid Driven OMM (**a**) EL degradation; (**b**) Schiffer factors; (**c**) Battery degradation.

Hence, the strategy proposed in this paper is able to offer an extension of the remaining useful life that can be higher than 10%. Of course these results could be confronted with real data, and with membrane post-mortem analysis, allowing to calibrate the real life duration of the devices, and use such statistics as MTBF (mean time between failures) or other indicators as proposed in [3]. However, this requires a very heavy experimental work, which is beyond the topic of the paper.

6. Conclusions

A dynamic hybrid system is characterised by several operating modes. Each operating mode groups together a set of services provided by a subset of system components, enabling the achievement of the objectives associated to the modes. Several factors can modify the behaviour of the system over time. There are at least three. The first is a voluntary modification by the user of the objectives to be achieved by the system. This results in the definition of new values for the system outputs. The second is related to an uncontrolled modification of the values of the system inputs. The trajectories must then be adapted to guarantee the non-modification of the expected outputs. The third is linked to the modification of a physical law associated with a component following the total or partial failure of that component. This modification must be compensated by using other components. In this case, reconfiguration solutions must exist.

To take into account these multiple operating possibilities, Event-Driven operating mode management is generally proposed. This method is based on instantaneous data and ensures that the system fulfills its mission with the required quality, in complete safety.

The new approach developed in this paper is based on the principle that even if there is a degree of indeterminacy concerning the environment in which the system operates, the temporal evolution of its inputs and outputs is never totally unknown. In many cases, it can be predicted. It then becomes possible to propose a management of operating modes based on both predictive and event data. Based on these predictive data, the optimal sequence of operating modes that minimizes or maximizes a set of criteria can then be proposed. In the presented work, it has been chosen to maximize the lifetime of the most expensive components in a system.

The results obtained by applying the proposed theoretical approach to a hydrogen production system demonstrate the relevance of the proposed approach.

Author Contributions

R.A.: methodology, software, writing—original draft preparation, A.-L.G., methodology, writing—original draft preparation, supervision, J.-Y.D., writing—review and editing, supervision, funding acquisition. All authors have read and agreed to the published version of the manuscript.

Funding

This work received no external funding.

Institutional Review Board Statement

Not applicable.

Informed Consent Statement

Not applicable.

Data Availability Statement

No data are available.

Conflicts of Interest

The authors declare no conflict of interest.

References

1. Chatti, N.; Gehin, A.-L.; Ould-Bouamama, B.; et al. Functional and behavior models for the supervision of an intelligent and autonomous system. *IEEE Trans. Autom. Sci. Eng.* **2013**, *10*, 431–445. [CrossRef]
2. Gehin, A.-L.; Staroswiecki, M. Reconfiguration analysis using generic component models. *IEEE Trans. Syst. Man Cybern. A Syst. Hum.* **2008**, *38*, 575–583.
3. Watanabe, A.T.; Sebem, R.; Leal, A.B.; et al. Fault prognosis of discrete event systems: An overview. *Annu. Rev. Control* **2021**, *51*, 100–110.
4. Arunthavanathan, R.; Khan, F.; Ahmed, S.; et al. An analysis of process fault diagnosis methods from safety perspectives. *Comput. Chem. Eng.* **2021**, *145*, 107197.
5. Venkatasubramanian, V., Rengaswamy, R., Yin, K., et al. A review of process fault detection and diagnosis: Part i: Quantitative model-based methods. *Comput. Chem. Eng.* **2003**, *27*, 293–311. [CrossRef]
6. Reiter, R. A theory of diagnosis from first principles. *Artif. Intell.* **1987**, *32*, 57–95. [CrossRef]
7. Pulido, B.; Gonzalez, C.A. Possible conflicts: a compilation technique for consistency-based diagnosis. *IEEE Trans. Syst. Man Cybern. B Cybern.* **2004**, *34*, 2192–2206.
8. Meng, Q.; Yang, H.; Jiang, B.; et al. Accessibility, observability, and fault-tolerant control structure selection of network nonlinear systems. *IEEE Trans. Control Netw. Syst.* **2022**, *9*, 75–87.
9. Trapiello, C.; Puig, V.; Cembrano, G. Reconfiguration of large-scale systems using back-up components. *Comput. Chem. Eng.* **2021**, *149*, 107288.
10. Van der Schaft, A.J.; Schumacher, J.M. Modelling and analysis of hybrid dynamical systems. In *Advances in the Control of Nonlinear Systems*; Banos, A., Lamnabhi-Lagarrigue, F., Montoya, F.J., Eds.; Springer: London, UK, 2001; pp. 195–224.
11. Yu, M.; Xiao, C.; Zhang, B. Event-triggered discrete component prognosis of hybrid systems using degradation model selection. *IEEE Trans. Ind. Electron.* **2020**, *68*, 11470–11481.
12. Connolly, C.; Taylor, K.; Bankhead, M.; et al. Techno-Economic Analysis of Heat-Assisted Hydrogen Production from Nuclear Power. *New Energy Exploit. Appl.* **2024**, *3*, 108–129. [CrossRef]
13. Abdallah, I.; Gehin, A.-L.; Ould Bouamama, B. Event driven hybrid bond graph for hybrid renewable energy systems part i: Modelling and operating mode management. *Int. J. Hydrogen Energy* **2018**, *43*, 22088–22107. [CrossRef]
14. Krishnan, S., Koning, V., Theodorus de Groot, M., et al. Present and future cost of alkaline and pem electrolyser stacks. *Int. J. Hydrogen Energy* **2023**, *48*, 32313–32330. [CrossRef]
15. Šimunović, J.; Radica, G.; Barbir, F. The effect of components capacity loss on the performance of a hybrid PV/wind/battery/hydrogen stand-alone energy system. *Energy Convers. Manag.* **2023**, *291*, 117314.
16. Liberzon, D. *Switching in Systems and Control*; Birkhauser: Boston, MA, USA, 2012; pp. 1–12.
17. Tuntas, R.; Hames, Y. Modeling of switching systems with artificial neural networks. *J. Appl. Sci.* **2005**, *5*, 1232–1236.
18. Abdallah, I.; Gehin, A.-L.; Ould Bouamama, B. Event driven hybrid bond graph for diagnosis. In Proceedings of the 2016 European Control Conference, Aalborg, Denmark, 29 June–1 July 2016.
19. Bouchebbat, R.; Gherbi, S. A novel optimal control and management strategy of stand-alone hybrid pv/wind/diesel power system. *J. Control Autom. Electr. Syst.* **2017**, *28*, 284–296.
20. Sood, S.; Prakash, O.; Dieulot, J.Y.; et al. Robust diagnosis of PEM electrolysers using LFT bond graph. *Int. J. Hydrogen Energy* **2022**, *47*, 33938–33954.
21. Sood, S.; Prakash, O.; Boukerdja, M.; et al. Generic dynamical model of PEM electrolyser under intermittent sources. *Energies* **2020**, *13*, 6556.
22. Belkacem, L.; Simeu-Abazi, Z.; Dhouibi, H.; et al. Diagnostic and prognostic of hybrid dynamic systems: Modeling and RUL evaluation for two maintenance policies. *Reliab. Eng. Syst. Saf.* **2017**, *164*, 98–109. [CrossRef]
23. El Kafazi, I.; Bannari, R.M. Multiobjective scheduling-based energy management system considering renewable energy and energy storage systems: a case study and experimental result. *J. Control Autom. Electr. Syst.* **2019**, *30*, 1030–1040. [CrossRef]
24. Ghane-Kanafi, A.; Khorram, E. A new scalarization method for finding the efficient frontier in non-convex multi-objective problems. *Appl. Math. Modell.* **2015**, *39*, 7483–7498. [CrossRef]
25. Marler, R.T.; Arora, J.S. The weighted sum method for multi-objective optimization: new insights. *Struct. Multidiscip. Optim.* **2010**, *41*, 853–862. [CrossRef]
26. Dufo-López, R. Off-grid full renewable hybrid systems: Control strategies, optimization, and modeling. In *Hybrid Technologies for Power Generation*; Lo Faro, M., Barbera, O., Giacoppo, G., Eds.; Academic Press: Cambridge, MA, USA. pp. 69–100.

27. Oliveira, D.Q.; Saavedra, O.R.; Santos-Pereira, K.; et al. A critical review of energy storage technologies for microgrids. *Energy Syst.* **2021**, 1–30.
28. Nguyen, M.Y.; Nguyen, D.H.; Yoon, Y.T. A new battery energy storage charging/discharging scheme for wind power producers in real-time markets. *Energies* **2012**, *5*, 5439–5452. [CrossRef]
29. Santos-Pereira, K.; Pereira, J.D.; Veras, L.S.; et al. The requirements and constraints of storage technology in isolated microgrids: A comparative analysis of lithium-ion vs. lead-acid batteries. *Energy Syst.* **2021**, 1–24. [CrossRef]
30. Schiffer, J.; Sauer, D.U.; Bindner, H.; et al. Model prediction for ranking lead-acid batteries according to expected lifetime in renewable energy systems and autonomous power-supply systems. *J. Power Sources* **2007**, *168*, 66–78. [CrossRef]
31. Bashir, N.; Sardar, H.S.; Nasir, M.; et al. Lifetime maximization of lead-acid batteries in small scale ups and distributed generation systems. In Proceedings of the 2017 IEEE Manchester PowerTech, Manchester, UK, 18–22 June 2017.
32. Arsad, A.Z.; Hannan, M.A.; Al-Shetwi, A.Q.; et al. Hydrogen electrolyser technologies and their modelling for sustainable energy production: A comprehensive review and suggestions. *Int. J. Hydrogen Energy* **2023**, *48*, 27841–27871.
33. Xu, B.; Ma, W.; Wu, W.; et al. Degradation Prediction of Pem Water Electrolyzer Under Constant and Start-Stop Loads Based on Cnn-Lstm. *Energy AI* **2024**, *18*, 100420.
34. Chandesris, M.; Médeau, V.; Guillet, N.; et al. Membrane degradation in PEM water electrolyzer: Numerical modeling and experimental evidence of the influence of temperature and current density. *Int. J. Hydrogen Energy* **2015**, *40*, 1353–1366.
35. Kuhnert, E.; Mayer, K.; Heidinger, M.; et al. Impact of intermittent operation on photovoltaic-PEM electrolyzer systems: A degradation study based on accelerated stress testing. *Int. J. Hydrogen Energy* **2024**, *55*, 683–695.
36. Abdallah, R.; Gehin, A.-L.; Dieulot, J.-Y. Battery lifetime optimization in a solar microgrid. In Proceedings of the 2022 IEEE 17th international conference on control and automation, Naples, Italy, 27–30 June 2022.
37. Jangdoost, A.; Keypour, R.; Golmohamadi, H. Optimization of distribution network reconfiguration by a novel RCA integrated with genetic algorithm. *Energy Syst.* **2021**, *12*, 801–833. [CrossRef]